# Hydrostatic pressure effects on Raman spectra and the fundamental absorption edge in $2H$-$PbI_2$ crystals

A. Saitoh, T. Komatsu, and T. Karasawa
*Department of Physics, Osaka City University, Sumiyoshi-ku, Osaka 558-8585, Japan*
(Received 10 May 1999; revised manuscript received 27 December 1999)

The pressure dependence of the Raman and luminescence spectra of $2H$-$PbI_2$ has been studied under hydrostatic pressure up to 1.5 GPa at 77 K by using a diamond-anvil cell. A structural phase transition occurs at a pressure of $P_{PT}=0.56\pm0.01$ GPa. From the analysis of the Raman spectra, it is proposed that the unit cell of the high-pressure phase is a $2\times2$ supercell of that of the low-pressure phase. The peak energies of the free exciton recombination and donor-acceptor pair bands shift continuously across the phase transition, indicating that relative positions of atoms and the nature of interatomic bonding hardly change at the phase transition. The pressure dependence of the fundamental absorption edge which is well described by the Urbach rule has also been examined at 77 and 300 K. At $P_{PT}$ the steepness constant $\sigma_0$ in the Urbach tail changes drastically from 1.70 to 0.63. This result is consistent with the proposed doubling of unit-cell dimensions at $P_{PT}$.

## I. INTRODUCTION

In typical direct-gap layered semiconductors, intense exciton transitions appear at the fundamental absorption edge. Exciton transition spectra are characterized by the oscillator strength and the exciton-phonon interaction strength. The lattice relaxation energy of the excitons is governed by their bandwidths as well as the coupling strengths between excitons and phonons. Therfore the application of hydrostatic pressure to layered materials is expected to result in major changes in transition spectra of excitons interacting with phonons.

In some layered crystals, such as $BiI_3$, the intensity of a photoluminescence from a self-trapped exciton (STE) state diminishes with increasing hydrostatic pressure.[1] This indicates an instability of the STE states under pressure. In $PbI_2$ at atmospheric pressure, the Urbach steepness constant connecting directly with the exciton-phonon coupling strength has a value 1.67 (Ref. 2) near the threshold at which the free exciton (FE) band bottom and the STE state invert their minimum energies,[3] as it has in $BiI_3$ crystals under pressure.

The $PbI_2$ single crystals have various polytypes under atmospheric pressure. The simplest structure is of the $2H$ type and belongs to the space group $D_{3d}^3$. Its hexagonal unit cell, which in terms of $x$, $y$, and $z$ coordinates is defined by the three basis vectors

$$a=\begin{pmatrix}\sqrt{3}a_0/2\\ -a_0/2\\ 0\end{pmatrix},\quad b=\begin{pmatrix}0\\ a_0\\ 0\end{pmatrix},\quad c=\begin{pmatrix}0\\ 0\\ c_0\end{pmatrix},$$

with the lattice constants $a_0=4.555$ Å, and $c_0=6.977$ Å,[4] contains one molecule. Layers of I-Pb-I are stacked along the $c$ axis. Each layer is tightly held together by strong covalent-ionic bonds. The weak interlayer forces between neighboring atomic sheets of iodines are generally ascribed to the van der Waals interaction.

Because of the highly anisotropic bonding, layered crystals often exhibit relatively large changes in the electronic structure under hydrostatic pressure. Many investigations have been reported on the optical properties in $PbI_2$. Concerning the hydrostatic pressure effects on $PbI_2$ crystals, however, very few experimental data have been reported yet.[5,6] Jayaraman *et al.*[5] performed the experiments in $PbI_2$ on the pressure dependence of the Raman lines at room temperature. They reported the phase transition pressure of 0.5 GPa in $2H$ polytype as evidenced by the appearance of new Raman lines, and proposed a monoclinic or a tetragonal $ZrO_2$-type structure after the phase transition. There has been no literature on high-pressure x-ray studies of the crystal structure after the phase transition.[7] Carillon and Martinez[6] measured the pressure coefficient of the absorption edge in $2H$-$PbI_2$ at 78 K. They reported that the phase transition occurs at 0.4 GPa because of a clear decrease in the absorption coefficient. The structural change as well as the electronic structure in $PbI_2$ under hydrostatic pressure has not been fully understood yet.

Our motivation is to clarify how hydrostatic pressure controls the unit-cell volume in anisotropic crystals, particularly for $PbI_2$, a typical layered material; and also to understand how the electronic states and exciton-phonon interaction depend on pressure. To this end, we measured the Raman spectra, the absorption-tail spectra of the exciton band, and the luminescence spectra of $2H$ polytype crystals under pressure. This data is used to show that the high-pressure unit cell of $PbI_2$ is a $2\times2$ supercell of the low-pressure phase.

## II. EXPERIMENT

$PbI_2$ single crystals were grown from the vapor. Then their crystal structure and quality were examined by x-ray diffraction and optical measurements of Raman and luminescence spectra. Only the best quality crystals were used; their typical thickness was about 0.07 mm.

For the optical measurements, we used a cryostat with a diamond-anvil cell under hydrostatic pressure at 77 K. A chamber made of a pair of coaxial bellows and containing high-pressure helium gas controlled the pressure on the

 

sample. More experimental details are in our previous paper.[8]

The pressure dependence of the Raman spectra was observed in the backscattering geometry. The incident light was the 6328-Å line from a He-Ne laser; the scattering light was analyzed by a double monochromator (Jobin Yvon model U-1000) and detected with a photomultiplier tube (Hamamatsu Photonics model R-928). Raman spectra at many pressures around the phase transition were measured to better define the phase-transition pressure.

Luminescence spectra were measured with the same apparatus as for the Raman measurements, except the incident light was the 4880-Å line of an argon ion laser. After all liquid helium evaporated, the temperature dependence of the luminescence spectra was measured while the sample warmed from 4.2 K. The crystal temperature was measured by an AuFe-chromel thermocouple attached to a gasket.

A two-beam method was used to measure the pressure dependence of the absorption spectra at 290 and 77 K. In this method, the incident light was split with a half mirror into two beams; one passed through the cell while the other passed through a pinhole outside the cryostat. The absorption intensity was determined from the intensity ratio of the two beams.

The crystals were put in the phosphor-bronze gasket hole after cutting them to the proper size with a razor. Both the thickness of the gasket and the hole diameter were 0.50 mm. For the absorption-spectrum measurements, we used a gasket with a 0.2 mm diameter hole on the bottom and one of 0.5 mm diameter on top such that the sample fit inside the larger hole and rested on the smaller. This prevented stray light from passing around the edge of the crystal: all of the light in the measurements was transmitted through the crystal. A 4:1 methanol-ethanol mixture and liquid nitrogen were used as pressure media at 300 and 77 K, respectively. The transmitted light intensity did not change; this indicates that the fluids did not solidify. The pressure was measured from the spectral shift of the $R_1$ luminescence line of a ruby crystal put in a separate gasket hole near the sample.[9] The width of the $R_1$ luminescence line did not change at 300 and 77 K over the pressure range studied, showing that the pressure is homogeneous and hydrostatic.

## III. RESULTS AND DISCUSSION

### A. Raman spectra under hydrostatic pressure

Figure 1 has the Raman spectra (Stokes lines) at 77 K and pressures up to 1.22 GPa. The lowest spectrum, 0 GPa (atmospheric pressure), has peaks at 78 and 98 $cm^{-1}$; the spectral line labeled P is a plasma line of the He-Ne laser. The $2H$-$PbI_2$ crystal has the following normal modes: $\Gamma = A_{1g} + E_g + 2A_{2u} + 2E_u$. The peaks at 78 and 98 $cm^{-1}$ are attributed to the Raman active modes $E_g$ and $A_{1g}$, respectively. The $E_g$ and $A_{1g}$ modes represent intralayer optical vibrations with displacement vectors normal and parallel to the $c$ axis, respectively. One $A_{2u}$ and one $E_u$ mode correspond to the longitudinal acoustic (LA) and doubly degenerate transverse acoustic (TA) mode, respectively. The other two optical *ungerade* modes, $A_{2u}$ and $E_u$, are infrared active. At 0.57 GPa, the number of lines increases abruptly from 2 to 14, which indicates a structural phase transition. Near 0.57 GPa, Raman shifts of the $E_g$ and $A_{1g}$ modes do not change significantly, but the intensity of the $E_g$ mode increases above 0.57 GPa. When the applied pressure was fully released, the same Raman spectrum as that at 0 GPa reappeared with the initial intensities and energy positions: the transformation was reversible.

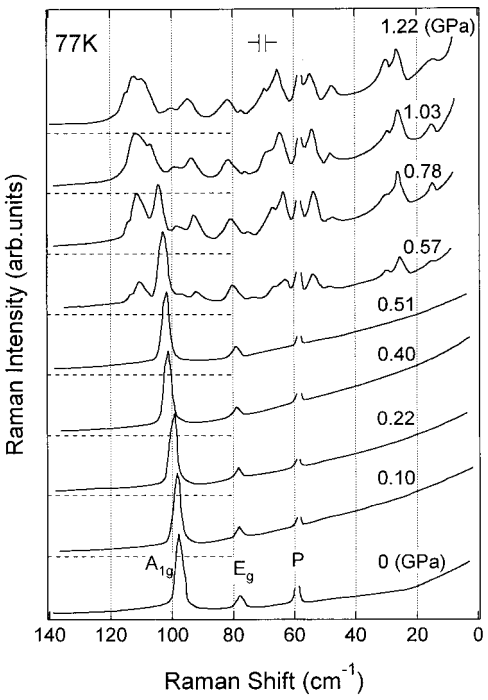


FIG. 1. Raman spectrum of $2H$-$PbI_2$ at 77 K at different pressures. The measurements used the backscattering geometry with the 6328-Å line of a He-Ne laser. P is a plasma line of the laser.

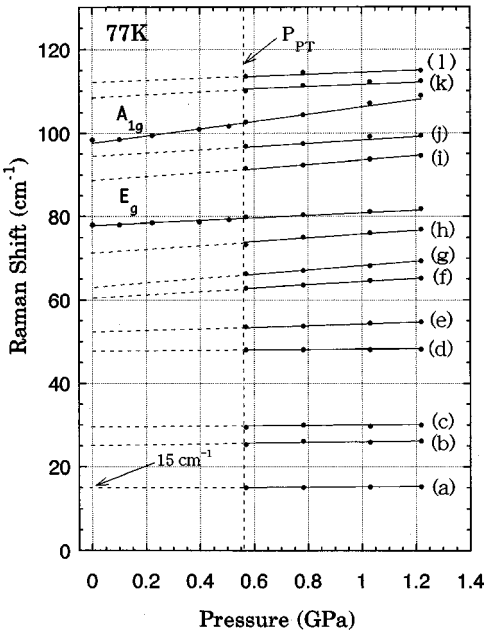


FIG. 2. Pressure dependence of the peak frequencies of the Raman spectra. A structural phase transition occurs at $0.56 \pm 0.01$ GPa as shown by the vertical dashed line. Dashed lines in the lower pressure side are extrapolations from Raman shifts in the higher pressure region. From these, we estimated the frequencies of the Raman lines at 0 GPa.

TABLE I. Frequencies and mode assignments of the Raman lines in $PbI_2$. Column one shows the extrapolated Raman frequencies at 0 GPa from those observed in the high-pressure phase in this work. In column 5, the mode symmetries corresponding to column one in the $2H$ polytype at the $\Gamma$ point are shown; e.g., $E_g[K]$ denotes the energy position at the $K$ point in the dispersion curve having the $E_g$ symmetry at the $\Gamma$ point. The unit of Raman shifts is $cm^{-1}$.

| This work Line 77 K | Neutron scattering in $2H$ (Ref. 10) (symmetry point) 298 K | Raman shifts of polytypes (Ref. 11) 50 K | Force-constant model in $2H$ (Ref. 11) 50 K | Mode in $2H$ at the $\Gamma$ point |
|---|---|---|---|---|
| | | 11.8($8H$) | | |
| | | 13.8($6H$) | | |
| *a* 15 | 14.9($A$) | 15.2($4H$) | | TA |
| *b* 25 | 23.0($K$) | | | TA |
| *c* 29 | 29.4($A$) | | | LA |
| *d* 47 | 46.1($K$) | | | LA, TA |
| *e* 52 | 53.3($\Gamma$) | | | $E_u$(TO) |
| *f* 60 | 58.3($A$) | | | $E_u$(TO)[$A$] |
| *g* 64 | 64($K$)[a] | | | $E_g[K]$ |
| *h* 71 | | 74.6($4H$) | 75($A$) | $E_g[A]$ |
| $E_g$ 78 | | 77.5($2H$) | 78($\Gamma$) | $E_g$ |
| 78 | 78.1($K$) | | | $E_u$(LO)[$K$] |
| *i* 88 | | | 87($A$) | $A_{1g}[A]$ |
| *j* 94 | 94($K$)[a] | | | $E_u$(TO)[$K$] |
| $A_{1g}$ 98 | | 97.3($2H$) | 97($\Gamma$) | $A_{1g}$ |
| *k* 109 | | 111.1($2H$) | 111($\Gamma$) | $A_{2u}$(LO) |
| *l* 112 | | | 115($A$) | $A_{2u}$(LO)[$A$] |

[a]Extrapolated values at the $K$ point from the measured data points in Ref. 10.

The observed Raman frequencies are plotted versus pressure in Fig. 2. From these experiments, the phase transition pressure $P_{PT}$ was determined to be $0.56 \pm 0.01$ GPa, which is close to the phase transition pressure of 0.5 GPa at room temperature measured by Jayaraman *et al.*[5] However, they observed only eight Raman lines in the higher-pressure region at room temperature compared to our 14; this is probably because weak Raman lines are more difficult to resolve at the higher temperature of their measurements. As the pressure increases above 0.56 GPa, each of these 14 Raman lines shifts toward higher frequencies in proportion to the pressure (Fig. 2). Even above 0.56 GPa, the $E_g$ and $A_{1g}$ modes remain. The frequencies of the two lines do not have a discontinuous change at $P_{PT}$, and moreover, each of the pressure coefficients of the two lines does not change at $P_{PT}$.

The possible structure of the high-pressure phase is discussed as follows. The 12 Raman lines that are only above $P_{PT}$ are divided into two groups according to their Raman shifts as follows: the first group are those close to the $A_{1g}$ mode and are labeled (i) through (l) in Fig. 2, those in the second group all have frequencies below the optical phonon mode $E_g$, which has the lowest frequency in the pressure region below $P_{PT}$, and are labeled (a) through (h). This second group has frequencies corresponding to the acoustic branches at atmospheric pressure. These facts suggest that the new Raman lines arise from a folding-back of the phonon branches in the Brillouin zone (BZ) of $2H$ polytype (the fundamental BZ). Therefore we argue that the new unit cell is made up of several unit cells of $2H$ polytype. Because the frequencies and pressure coefficients of the $E_g$ and $A_{1g}$ modes do not change discontinuously at $P_{PT}$, the relative positions of atoms, interatomic bonding, and interatomic force constants hardly change at the phase transition. Consequently, the phonon dispersion curves in the folded-back BZ hardly change their energies from those in the corresponding fundamental BZ.

The phonon dispersion curves of $PbI_2$ measured at 0 GPa and those of the $2H$ polytype calculated using the force-constant model were reported in Refs. 10 and 11. By comparing the frequencies of these phonon dispersion curves at the zone center or edges with those of the above 12 Raman lines in this work, we deduced some properties of the enlarged unit cell. Raman lines (a)–(l) have constant pressure coefficients above $P_{PT}$ that are used to extrapolate their frequencies to 0 GPa in Fig. 2.

Table I shows those values in the first column and includes the frequencies of the $E_g$ and $A_{1g}$ modes. For example, the extension of the lowest straight line denoted by (a) intersects the vertical line of 0 GPa at 15 $cm^{-1}$ in frequency as seen in Fig. 2. The phonon dispersion curves of $2H$ polytype measured by the neutron scattering were reported by Dorner *et al.*[10] The frequencies of these phonon dispersion curves at the $\Gamma$, $A$, and $K$ points are listed in the second column in Table I. These frequencies agree with some of our results in the first column. For example, the frequency of the TA mode at point $A$ is 14.9 $cm^{-1}$ from the second column; this coincides with the extrapolated frequency 15 $cm^{-1}$ of the Raman line denoted by (a) in the first column. Phonon dispersion curves determined by the Raman spectra of several polytypes and calculated from the force-constant model were reported by Sears *et al.*[11] The results are listed in columns 3 and 4 of Table I. The Raman

frequencies of $2H$ and $4H$ polytypes in column three and the frequencies at the $\Gamma$ and $A$ points under column four correspond to other results in column one. Thus Raman frequencies (a), (c), (f), (h), (i), and (l) are likely from the new modes at the $\Gamma$ point in the new BZ with values from those at the $A$ point of branches TA, LA, $E_u$(TO), $E_g$, $A_{1g}$, and $A_{2u}$(LO), respectively. The latter are in the fundamental BZ. This is because of the doubling of the lattice constant of the new unit cell along the $c$ axis corresponding to the $\Gamma$-$A$ direction. These are listed in the last column of Table I. In column one of Table I, the frequencies of the lines denoted by (b), (d), (g), (j), and 78 $cm^{-1}$ approximately equal those at the $K$ point given in column two. The $\Gamma$-$K$ direction in the fundamental BZ corresponds to the direction along the $b$ axis in real space. Hence the new unit cell also has a doubling of the lattice constants along both the $b$ and $c$ axes. Consequently, the new unit cell is made up of four unit cells of $2H$ polytype. The intensity of the Raman line assigned as $E_g$ (78 $cm^{-1}$ at 0 GPa) abruptly increases above $P_{PT}$ with increasing pressure (Fig. 1); this suggests that for pressures above $P_{PT}$, the folded mode (78.1 $cm^{-1}$) from the $K$ point in the fundamental BZ nearly superimposes on the $E_g$ mode. The frequencies of lines $e$ and $k$ in column 1 (52 and 109 $cm^{-1}$) are close to those of the *ungerade* modes $E_u$(TO) (53.3 $cm^{-1}$) and $A_{2u}$(LO) (111.1 $cm^{-1}$) at the $\Gamma$ point in the fundamental BZ, respectively. The two *ungerade* modes probably become *gerade* modes in the high-pressure phase because of the extension of the unit cell resulting in the observation of them as the Raman-active modes.

### B. Pressure dependence of the steepness constant

The extension of the unit-cell volume also affects the transition spectra of the bulk exciton state by changing the exiton-phonon interaction. In Fig. 3, the pressure dependence of the fundamental absorption edge with incident light parallel to the $c$ axis is shown for 77 K (●) and 290 K (○); the ordinate shows the optical density (OD) on a logarithmic scale. The figure shows that the absorption tails closely follows Urbach's rule at all pressures.[12] As pressure increases, the absorption tails shift to lower energy and their gradients decrease at both temperatures. When the applied pressure is released, the absorption spectra coincide with those obtained initially at 0 GPa at both temperatures. Therefore structural defects do not affect these spectra even at high pressure.

The steepness factor $\sigma$ is

$$\sigma = \sigma_0 \left( \frac{2k_B T}{\hbar \omega_P} \right) \tanh \left( \frac{\hbar \omega_P}{2k_B T} \right), \tag{1}$$

where the steepness constant $\sigma_0$ is the high-temperature limit of $\sigma$, and $\hbar\omega_P$ is the effective phonon energy. The value of the steepness constant $\sigma_0$ is a criteria for exciton self-trapping.[13]

Figure 4 shows the pressure dependence of $\sigma$ at 77 K (●) and 290 K (○). At 77 K, $\sigma$ decreases slightly from 1.41 at 0 GPa to reach 1.39 just below $P_{PT}$. When the pressure reaches $P_{PT}$, $\sigma$ jumps down to 0.52 and thereafter decreases to 0.46 as the pressure increases to 1.5 GPa. At 290 K, $\sigma$ also drops near $P_{PT}$; extrapolating, $\sigma$ increases from 1.65 at 0 GPa to near 1.67 just below $P_{PT}$, drops to approximately 0.62 at $P_{PT}$, and then decreases to near 0.56 at 1.5 GPa.

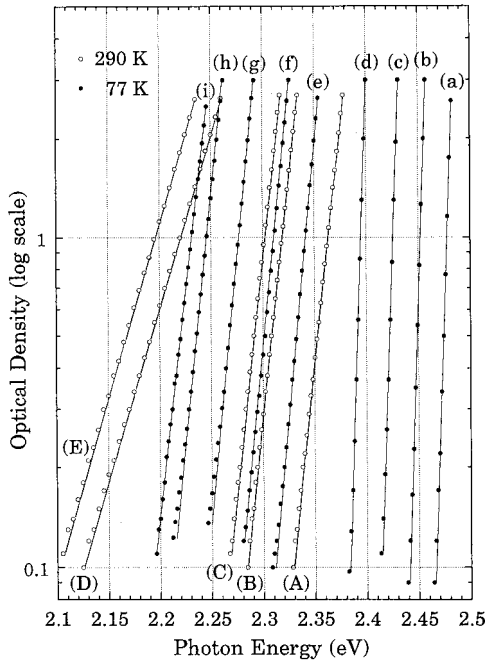


FIG. 3. Pressure dependence of the absorption spectrum near the absorption edge at 77 K (●) and the following pressures: (a) 0 GPa, (b) 0.219 GPa, (c) 0.333 GPa, (d) 0.552 GPa, (e) 0.697 GPa, (f) 1.06 GPa, (g) 1.25 GPa, (h) 1.65 GPa, and (i) 2.08 GPa. Similarly for 290 K (○) and the following pressures: (A) 0 GPa, (B) 0.23 GPa, (C) 0.34 GPa, (D) 0.85 GPa, and (E) 0.96 GPa.

Using Eq. (1) and the $\sigma$ data at 77 and 290 K for the four different pressures, we calculated the four curves shown in

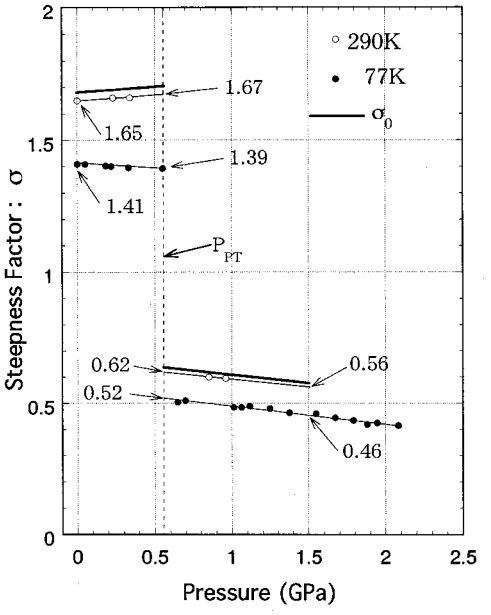


FIG. 4. Pressure dependence of the steepness factor at 77 K (●) and 290 K (○). The vertical broken line indicates the phase transition pressure $P_{PT}$. When the pressure reaches $P_{PT}$, the $\sigma$ value jumps from 1.67 down to 0.62 at 290 K, and from 1.39 down to 0.52 at 77 K. The heavy solid line shows the pressure dependence of $\sigma_0$.

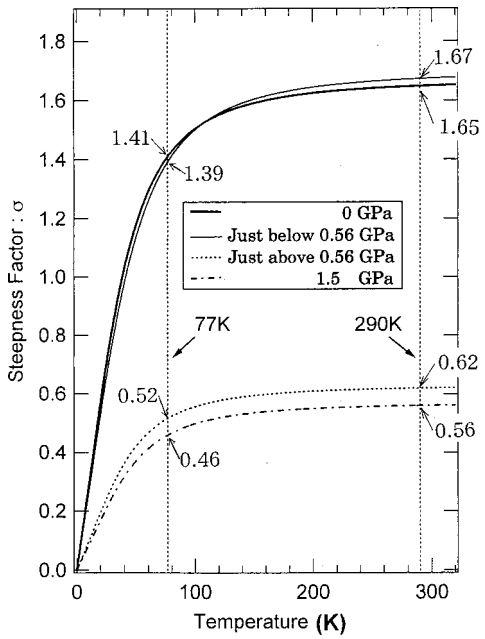


FIG. 5. Temperature dependence of the steepness factor $\sigma$. The heavy solid, light solid, dotted, and dashed-dotted curves show the theoretical curves at 0 GPa, just below 0.56 GPa, just above 0.56 GPa, and at 1.5 GPa, respectively. The vertical broken lines indicate the temperatures of 77 and 290 K.

Fig. 5; the heavy solid, light solid, dotted, and dashed-dotted curves are $\sigma$ at 0 GPa, just below $P_{PT}$, just above $P_{PT}$, and at 1.5 GPa, respectively. The values of $\sigma_0$ and $\hbar\omega_P$ in Table II for the four pressures were obtained from these curves. The values of $\sigma_0$ of 1.67 and $\hbar\omega_P$ of 10 meV at 0 GPa agree with previous estimates.[14] $\sigma_0$ decreases abruptly from 1.70 to 0.63 at $P_{PT}$, but $\hbar\omega_P$ (11 meV) does not change significantly with pressure. The pressure dependence of $\sigma_0$ is shown by the heavy solid lines in Fig. 4. We consider now the reason why $\sigma_0$ jumps from the large to the small values at the phase transition. The steepness constant $\sigma_0$ is[3]

$$\sigma_0 = s\frac{B}{E_{LR}}, \tag{2}$$

where $s$, the steepness index, is determined by the crystal's dimensionality and structural symmetry, $B$ is the half-width of the exciton band, which equals twice the transfer energy, and $E_{LR}$ is the lattice relaxation energy. $E_{LR}$ depends on $\hbar\omega_P$ and the strength of the electron-phonon interaction;[15] the former did not change at $P_{PT}$ and we think that the latter does not significantly change at $P_{PT}$ because the nature of the interatomic bonding hardly changes at the phase transition (see Sec. III A). Therefore $E_{LR}$ is nearly constant across the phase transition. Furthermore, because the relative atomic positions do not significantly change at the phase transition, $s$ does not change at $P_{PT}$. Hence we conclude that the drastic change in $\sigma_0$ at $P_{PT}$ is due only to a change in $B$. The decrease in $B$ to nearly one-third of that at the phase transition can be understood as follows. The folding-back effect on the exciton band in the BZ by the extension of the unit-cell size in the high-pressure phase reduces the bandwidth. The doubling of the unit cell along the $b$ and $c$ axes reduces the BZ by one-half in the $\Gamma$-$K$ and $\Gamma$-$A$ directions, and the bandwidth in these directions will drop by more than one-half. According to electronic band calculations for $2H$-$PbI_2$,[16] the lowest conduction-band energy changes mostly along the $\Gamma$-$K$ direction. Hence $B$ would mostly be affected by the folding back of the exciton band along the $\Gamma$-$K$ direction.

TABLE II. Values of the steepness parameters at various pressures. $\sigma$ is the steepness factor at 77 and 290 K, $\sigma_0$ is the steepness constant, and $\hbar\omega_P$ is the effective phonon energy.

| Pressure (GPa) | $\sigma$ (77 K) | $\sigma$ (290 K) | $\sigma_0$ | $\hbar\omega_P$(meV) |
|---|---|---|---|---|
| 0 | 1.41 | 1.65 | 1.67 | 10 |
| Just below 0.56 | 1.39 | 1.67 | 1.70 | 11 |
| Just above 0.56 | 0.52 | 0.62 | 0.63 | 11 |
| 1.5 | 0.46 | 0.56 | 0.57 | 11.5 |

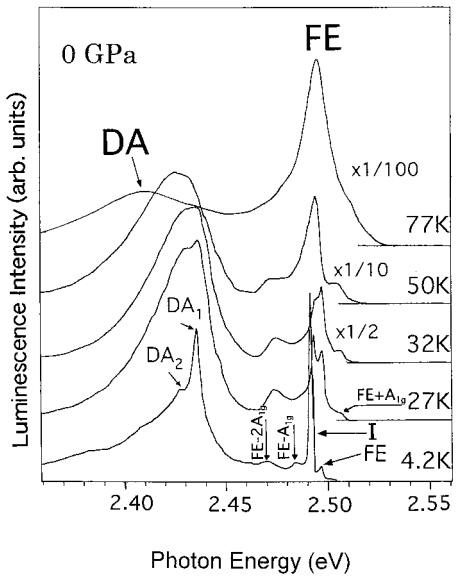


FIG. 6. Luminescence spectra of $2H$-$PbI_2$ excited with the 4880-Å line of an argon ion laser at several temperatures from 4.2 to 77 K and at atmospheric pressure. The FE band indicates recombination luminescence of the free exciton. The I indicates luminescence from impurity centers. FE$\pm A_{1g}$ and FE$-2A_{1g}$ are exciton recombinations associated with $A_{1g}$ phonons. $DA_1$ and $DA_2$ are D-A pair luminescence peaks. Spectra at higher temperatures have been amplified; for a direct comparison, they should be scaled by the factors shown.

### C. Pressure dependence of the luminescence spectra

Figure 6 shows the luminescence spectra in $2H$-$PbI_2$ at 0 GPa at several temperatures. The 4880-Å line of an argon ion laser was used as a source. The lowest spectrum at 4.2 K consists of exciton recombination lines and donor-acceptor (DA) pair bands; the line labeled FE at the highest energy is a direct recombination line of the free exciton, i.e., a recombination of an electron at the bottom of the conduction band and a hole at the top of the valence band at the $\Gamma$ point, line I is due to an exciton bound to a neutral donor;[17] whereas lines FE$-A_{1g}$ and FE$-2A_{1g}$ are the phonon-assisted bands of the exciton recombination with phonons $A_{1g}$ and $2A_{1g}$,

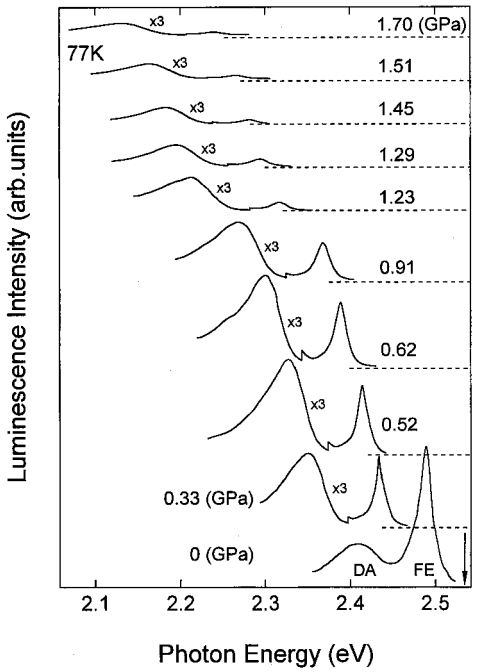


FIG. 7. Pressure dependence of the luminescence spectrum at 77 K. Above 0 GPa, the DA band is shown multiplied by 1/3. For a direct comparison to the higher energy peak, multiply by 3 as indicated by ''×3.'' The arrow indicates the source energy.

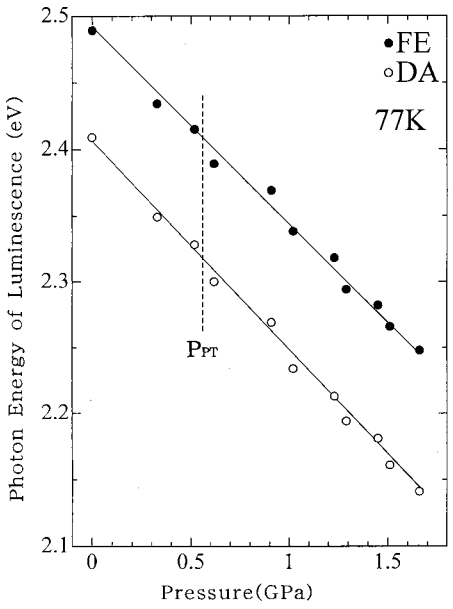


FIG. 8. Pressure-dependent the peak energies of the FE (●) and D-A pair luminescence (○) bands at 77 K. The vertical broken line indicates the phase transition pressure. Solid lines are the best fits to the data.

respectively. The donor-acceptor pair recombination bands $DA_1$ at 2.436 eV and $DA_2$ at 2.428 eV are the same as those reported by Bibik and Davydova.[18] With increasing temperature, the intensity of the luminescence becomes weaker above 27 K, and the I line transfers its intensity to that of the FE band. Although the intensity at 77 K is nearly two orders of magnitude less than that at 4.2 K, the band peaks of the FE recombination at 2.49 eV (Ref. 19) and DA recombination at 2.41 eV can be clearly resolved.

Figure 7 shows the pressure-dependent luminescence spectra at 77 K. The crystal was excited by an argon ion laser at 2.54 eV (4880-Å line). At 0 GPa, the excitation energy is larger than the FE energy by only 0.05 eV; hence the FE is generated directly by the source, which results in more intense FE luminescence than DA pair luminescence. The FE and DA peaks shift toward lower energies with increasing pressure. As a result, the same excitation light frequency increases the number of free electron-hole pairs over the FE exitons. Also, at 0.33 GPa, the intensity of the DA band increases, whereas the FE intensity decreases. At pressures above 0.62 GPa, the intensities of the FE and DA bands decrease gradually. This pressure region corresponds to the high-pressure phase with $\sigma_0$ less than 0.63. This is much smaller than the critical $\sigma_C$ value of 1.64,[3] where the state of minimum energy of the FE band competes with the STE state. Then, in the high-pressure phase, the FE state should become unstable and the STE state should be stable. Therefore the remarkable reduction of the FE and DA pair luminescence intensities is due to the instability of the FE state.[20]

The peak energies of the FE and DA bands are plotted as a function of pressure in Fig. 8. The shifts are proportional to the pressure in the whole pressure region with constant coefficients for the FE and DA bands of $-153$ and $-160$ meV/GPa, respectively. The negative pressure coefficients of the FE and DA bands originate mainly from the reduction of the band-gap energy with increasing pressure. The frequencies of the FE and DA bands do not jump at $P_{PT}$ probably because the band-gap energy does not significantly change at $P_{PT}$. This absence of a band-gap discontinuity is explained as follows. Because the relative positions of the atoms and interatomic bonding nature hardly change at the phase transition, the energies at conduction and valence-band extrema hardly change. Although the folding back at the phase transition affects the electronic band and produces small energy gaps at the folding-back point, the band-gap energy between the conduction and valence bands is nearly constant because neither the bottom of the conduction band nor the top of the valence band at the $\Gamma$ point change their energy.

## IV. CONCLUSION

The hydrostatic pressure dependence of the Raman spectra has been studied in $2H$-$PbI_2$ crystals at 77 K. At a pressure of $P_{PT}=0.56\pm0.01$ GPa, the number of Raman lines increases abruptly from 2 to 14, indicating a structural phase transition. The frequencies of the newly appearing Raman peaks correspond well to those of the phonon branches at the $K$ and $A$ points in the BZ of the $2H$-$PbI_2$. These results are interpreted in terms of zone-folding effects related to the formation of a $2\times2$ supercell along the basis vectors $b$ and $c$.

The absorption tail of the exciton transition in this crystal has been examined at room temperature and 77 K under the pressure. All of the tail spectra can be well fitted by an Urbach relation. When the pressure reaches $P_{PT}$, the value of the steepness constant $\sigma_0$ decreases discontinuously from 1.70 to 0.63. This extraordinary change in the $\sigma_0$ value is attributed to the abrupt reduction of the exciton bandwidth at the phase transition.

The photoluminescence of $PbI_2$ consists of the FE and DA bands. Both transitions shift to the lower energy with increasing pressure. The abrupt reduction of the exciton bandwidth and the absence of the band-gap discontinuity are consistently explained by zone-folding effects. In the pressure region above $P_{PT}$, the luminescence of the FE reduces remarkably its intensity corresponding to the reduction of the $\sigma_0$ value.

**ACKNOWLEDGMENTS**

The authors would like to thank Dr. I. Akai for his valuable advice, and Mr. Y. Nishitani for his help and cooperation in the experiments. This work was supported by a Grant-in-Aid for Scientific Reserch on Priority Areas, ''Photo-induced Phase Transition and Their Dynamics,'' from the Ministry of Education, Science, Sports and Culture of Japan.

[1] H. Kurisu, T. Komatsu, and T. Karasawa, J. Phys. Soc. Jpn. **62**, 1048 (1993).
[2] J. Takeda, T. Ishihara, and T. Goto, Solid State Commun. **56**, 101 (1985).
[3] M. Schreiber and Y. Toyozawa, J. Phys. Soc. Jpn. **51**, 1544 (1982).
[4] R. W. G. Wyckoff, *Crystal Structure*, 2nd. ed. (Interscience, New York, 1965), Vol. 1.
[5] A. Jayaraman, R.G. Maines, Sr., and T. Chattopadhyay, Pramana **27**, 449 (1986).
[6] C. Carillon and G. Martinez, Nuovo Cimento A **38**, 496 (1977).
[7] The x-ray-diffraction pattern of the high-pressure phase was similar to that of the $2H$-$PbI_2$ structure of the low-pressure phase. Hence, within the accuracy of the diffraction analysis, the atomic positions in the two phases are the same.
[8] H. Kurisu, T. Komatsu, T. Tanaka, I. Akai, T. Karasawa, and T. Iida, J. Lumin. **60&61**, 816 (1994).
[9] G.J. Piermarini, S. Block, J.D. Barnett,and R.A. Forman, J. Appl. Phys. **46**, 2774 (1975).
[10] B. Dorner, R.E. Ghosh, and G. Harbeke, Phys. Status Solidi B **73**, 655 (1976).
[11] W.M. Sears, M.L. Klein, and J.A. Morrison, Phys. Rev. B **19**, 2305 (1979).
[12] F. Urbach, Phys. Rev. **92**, 1424 (1953).
[13] M. Schreiber and Y. Toyozawa, J. Phys. Soc. Jpn. **52**, 318 (1983).
[14] T. Yao and I. Imai, Solid State Commun. **9**, 205 (1971).
[15] H. Hiramoto and Y. Toyozawa, J. Phys. Soc. Jpn. **54**, 245 (1985).
[16] I. Ch. Schlüter and M. Schlüter, Phys. Rev. B **9**, 1652 (1974).
[17] M.S. Skolnic and D. Bimberg, Phys. Rev. B **18**, 7080 (1978).
[18] V.A. Bibik and N.A. Davydova, Phys. Status Solidi A **126**, K191 (1991).
[19] R. Kleim and F. Raga, J. Phys. Chem. Solids **30**, 3313 (1969).
[20] The STE luminescence is expected to appear in the high-pressure phase. We examined the STE luminescence at 77 K from visible to infrared wavelengths using an InGaAs detector. However, these preliminary measurements gave no remarkable luminescence corresponding to the STE state in the high-pressure phase at energies down to 0.80 eV. Thus the nonradiative transition process suppresses this luminescence at 77 K or the detector was not sensitive enough.